Effects of Gas Adsorption on the Graphite-Supported Ag Nanoclusters: A Molecular Dynamics Study

ARTICLE *in* THE JOURNAL OF PHYSICAL CHEMISTRY C · DECEMBER 2013

Impact Factor: 4.77 · DOI: 10.1021/jp407626e

4 AUTHORS, INCLUDING:

Hamed Akbarzadeh
Hakim Sabzevari University
42 PUBLICATIONS **97** CITATIONS
SEE PROFILE

Hamzeh Yaghoubi
University of Tehran
4 PUBLICATIONS **21** CITATIONS
SEE PROFILE

Farid Taherkhani
Independent Researcher
35 PUBLICATIONS **129** CITATIONS
SEE PROFILE

THE JOURNAL OF PHYSICAL CHEMISTRY C

Article

pubs.acs.org/JPCC

Effects of Gas Adsorption on the Graphite-Supported Ag Nanoclusters: A Molecular Dynamics Study

Hamed Akbarzadeh,*[,†] Hamzeh Yaghoubi,[†] Amir Nasser Shamkhali,[‡] and Farid Taherkhani[§]

[†]Department of Chemistry, Faculty of Basic Sciences, Hakim Sabzevari University, Shahrak-e Towhid Street, 96179-76487 Sabzevar, Iran

[‡]Department of Chemistry, Faculty of Basic Sciences, University of Mohaghegh Ardabili, Daneshgah Street, 56199-11367 Ardabil, Iran

[§]Department of Physical Chemistry, Razi University, Tazeh Abad Street, 67149-67346 Kermanshah, Iran

ABSTRACT: Molecular dynamics simulations were used to investigate the adsorption effects of different gas phases on structural and dynamical properties of graphite-supported Ag nanoclusters at various pressures, temperatures, and cluster sizes. Three Ag nanoclusters with N = 38, 108, and 256 atoms in vacuum and under pressure of five gases (He, Ar, Xe, H_2, and CO) were simulated. The effect of each gas on nanoclusters at four temperatures and at various numbers of gas atoms (various pressures) was investigated. The adsorption, structural changes, and dynamic properties were monitored as a function of cluster size, pressure, and temperature. The adsorption isotherms, density profiles, deformation parameter, mean-square displacement, and diffusivity were calculated to study structural changes and dynamical properties of nanoclusters. It was found that the adsorption isotherms comply from the Langmuir type I. Also, the gas phase changes the vacuum cluster structure irreversibly. Furthermore, the gas phase increases the diffusivity of nanoclusters on the substrate surface, and this diffusivity increases with gas pressure.

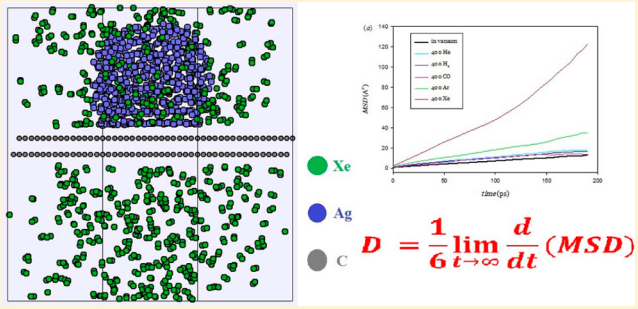

INTRODUCTION

Metallic nanoclusters are the subject of many experimental and theoretical researches due to their different physical, chemical, and electronic properties in comparison with the bulk material.[1,2] In most cases, these differences are related to their large fraction of surface atoms. Ag nanoclusters possess many valuable optical properties that have opened the door to new approaches in sensing and imaging applications, offering a wide range of detection modes such as colorimetric, scattering, surface enhanced Raman spectroscopy (SERS), and metal-enhanced fluorescence (MEF) techniques at extremely low detection limits.[3] In many cases of heterogeneous catalysis and sensors, the nanoclusters must be sited on a substrate, and gaseous reactants are adsorbed on those surface.[4] There is much evidence that emphasizes that the catalytic activity of nanoparticles is size- and shape-dependent.[5−7] Therefore, investigation of the dependency of the shape and structural changes of substrate-supported nanoclusters to the temperature and pressure of gas phase could give very important knowledge for a better understanding of their catalytic activity.

It is well-documented that the catalytic activity of a metal surface depends on its atomic structure.[8] The actual shape of an active catalyst is often thought to be related to the shape of clean particles observed by transmission electron microscopy (TEM) on model catalysts prepared in ultrahigh vacuum (UHV) conditions.[9] However, recent experiments are able to determine the structural and dynamic properties of metallic nanoclusters under more realistic conditions.[4,10]

Shape variations of Pd particles due to oxygen adsorption were investigated by Graoui et al.[11] They prepared Pd particles under UHV on MgO single crystals that were in situ annealed under various pressures of O_2 at high temperature, then observed ex situ via high-resolution transmission electron microscopy (HRTEM) and weak beam dark-field (WBDF) imaging. They found that the Pd particles (10−15 nm) reach the equilibrium shape after annealing in UHV at 550 °C (far below the melting point of Pd particles) because the atomic diffusion on the surfaces is fast enough for these particle sizes (<15 nm). Hansen et al. used TEM technique to study Cu nanocrystals supported on ZnO and silica substrates in contact with H_2O/H_2 and CO/H_2 gas mixtures.[4,12] They resulted that the structure of Cu nanoparticles is influenced by the nature of the substrate and gas atmosphere; also, reversible changes are strongly dependent on the nature of the gas phase.[4] Molecular simulation was carried out to investigate the adsorption of oxygen molecules on graphite-supported platinum clusters with different loadings at two temperatures by Wu et al.[4,13] The water adsorption mechanism on Au nanoparticles at different

Received: July 31, 2013
Revised: November 5, 2013
Published: November 8, 2013

sizes was investigated via molecular dynamics (MD) simulation by Ju.[14] It is found that the interaction energy between the Au nanoparticle and the water molecule is sensitive to the size of the Au nanoparticle, which has an obvious effect on the adsorption constant and the arrangement of the water molecules around the Au nanoparticles.

In this work, we have studied the effect of gas phase at various pressures, temperatures, and cluster sizes on graphite-supported Ag nanoclusters by MD simulation. Three Ag nanoclusters supported on graphite surface under pressure of five gases (He, Ar, Xe, H_2, and CO) were simulated for these aims.

CALCULATION METHOD

MD simulations were employed to study the gas phase on the structural and dynamical properties of the graphite-supported Ag nanoclusters. The MD simulations were carried out in the canonical ensemble (*NVT*) using Berendsen thermostat[15] with a relaxation time of 0.01 ps. A (39.35 × 34.08 × 60.7) ($Å^3$) cell of parallelepiped geometry was used in these simulations. Periodic boundary conditions were applied in the *x*, *y*, and *z* directions. Four temperatures (three of them below the melting point of nanoclusters and one of them above it) were considered to investigate the temperature dependence of adsorption. The equations of motion were integrated using the Verlet leapfrog algorithm[16] with time steps of 1 fs. The simulations were performed on nanoclusters with 38, 108, and 256 Ag atoms supported over a graphite substrate. The graphite was modeled as a two-layer carbon in ABAB arrangement with dimensions of 39.35 × 34.08 × 60.7 $Å^3$ and 1024 carbon atoms. Therefore, the graphite support is a bulk extended surface. The fcc nanocluster was placed 3 Å above the graphite surface. Then, the gas-phase atoms were initially distributed in the cell randomly. Therefore, the initial simulation box was composed of the cluster on the graphite and 400 gas atoms or molecules at random positions. Various gas pressures at constant volume and temperature were created by changing the number of gas atoms or molecules. So the pressure was reduced to near vacuum in several steps. At each step, 25% of gas atoms or molecules were removed, and after the end of each simulation, its output was used as the input for the next step. Five gases were used to represent the gas pressures: Ar, Xe, He, H_2, and CO. Simulation lengths of 400 ps for equilibration were followed by 800 ps for production time. All of the simulations were made by the DL_POLY 2.18 package.[17] Figure 1 shows a snapshot of the graphite-supported Ag_{256} nanocluster surrounded by 400 Xe at 300 K. (Note: Periodic boundary conditions were applied in three directions.)

In these simulations, pressure was calculated by van der Waals (VDW) equation of state for Ar, He, and Xe. For example, according to the conditions given in Figure 1, the Xe gas pressure is 71.5 atm. Also, an equation of state that was derived on the basis of the extended Lennard–Jones (12, 6, 3)[18] as the effective pair potential was chosen to calculate the pressure of CO and H_2.

The quantum Sutton–Chen (QSC) many-body potential[19] was applied for Ag–Ag interactions because this potential predicts the properties of fcc metallic clusters excellently. Also, this potential has been used in modeling the structural properties of metallic clusters in the size range of 13 to 309 atoms.[20] In the Sutton–Chen potential that is similar to the embedded atom model (EAM), the total internal energy of

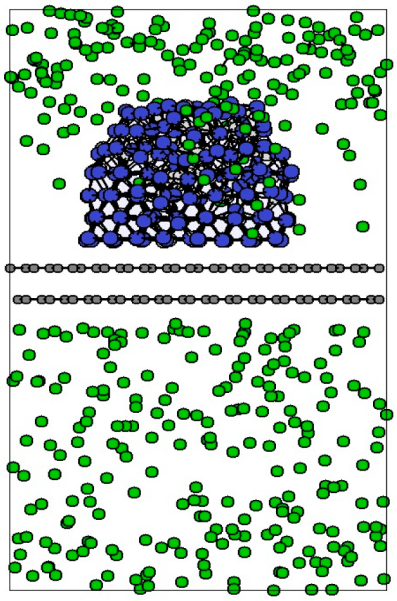

Figure 1. Snapshot of the graphite-supported Ag_{256} nanocluster surrounded by 400 Xe at 300 K.

pure metals was expressed in terms of Finnis–Sinclair form[21] as follows:

$$U_{\text{tot}} = \left[\frac{1}{2}\sum_{i\neq j}\sum_{j}\left(\frac{a}{r_{ij}}\right)^{n} - c\sum_{i}\rho_i^{1/2}\right] \quad (1)$$

The first term in eq 1 represents the pairwise repulsion between atomic cores, and the second term approximates the many-body metallic binding energy associated with the local electron density ρ_i:

$$\rho_i = \sum_{j\neq i}\left(\frac{a}{r_{ij}}\right)^{m} \quad (2)$$

Here r_{ij} is the spacing between atoms *i* and *j*, *c* is a positive dimensionless parameter, ε is a parameter with unit of energy, *a* is the lattice constant with the dimensions of length, and *m* and *n* are positive integer values ($n = m$). The parameters of QSC potential for Ag are ε = 0.033147 eV, *a* = 4.05 Å, *n* = 7, *m* = 6, and *c* = 16.399.

In these simulations, we considered two different force-field models for the graphite substrate:

(1) The carbon atoms of graphite were fixed in their positions (indeed we have a static surface).
(2) The optimized Tersoff potential[22] was applied for C–C interactions of graphite. The parameters of optimized Tersoff potential for graphite can be found in study of Lindsay and Broido.[22]

We compared the results obtained from the two models. There was no significant difference in results between the models (even at high temperatures and pressures). The reason is that the carbon support is a "bulk" extended surface, which will not be affected by the presence of the nanoclusters. We also ran several simulations considering larger sized graphite sheets; the results were similar to the first graphite system (because the graphite is a bulk surface). Therefore, we have reported the results obtained from the first model.

dx.doi.org/10.1021/jp407626e | J. Phys. Chem. C 2013, 117, 26287–26294

For the rest of interactions, we used the Lennard-Jones (L-J) 12−6 potential, for which the parameters are listed in Table 1.[23−27] CO and H_2 gases were considered as two-site models

Table 1. Lennard-Jones 12-6 Parameters Used in This Study[a]

interaction	ε (eV)	σ (Å)
Ag−Ag[25]	0.344700	2.644
C_g−C_g[25 b]	0.002630	3.369
He−He[26]	0.000900	2.550
Ar−Ar[26]	0.008000	3.540
Xe−Xe[26]	0.019900	4.050
H−H[27]	0.002383	2.640
O−O[24]	0.002601	3.120
C−C (for CO molecule)[24]	0.004553	3.430

[a]Ag−Ag and C_g-C_g parameters used only to calculate the other interactions by Lorentz−Berthelot rules (see text). [b]Subscript g denotes the graphite.

with fixed interatomic distance of 0.746 Å for H_2[23] and 1.163 Å for CO.[24] Also, the charges of C and O atoms in the CO molecule are +0.107 and −0.107 a.u., respectively.[24] The L-J parameters for dissimilar atoms were obtained by the Lorentz−Berthelot mixing rules. The columbic long-range interactions were calculated using the Ewald's method with a precision of 10^{-6}. All interatomic interactions between the atoms in the simulation box were calculated within the cutoff distance of 9 Å.

We used other potentials for Ag−CO and Ag−H_2 interactions and compared the results with the results obtained from the L-J potential. The Born−Mayer potential (B−M) was applied for Ag−CO interactions as the study of Spruit et al.[28] and Morse potential was applied for Ag−H_2 interactions as the study of Yu et al.[29] We ran several simulations considering these potentials for Ag−CO and Ag−H_2, obtaining results similar to those obtained from the L-J parameters. It represents physisorption in these systems. In this study, we have reported the results of the L-J potential for Ag−CO and Ag−H_2 gases.

To count the number of adsorbed gas atoms or molecules, we used the Ag-Gas radial distribution function (RDF). The position of the first peak in the RDF was chosen as a distance at which gas atoms were adsorbed. The first peak in Ag−gas RDF represents the first layer of adsorbed gases that were located around the Ag naonocluster. Therefore, the number of adsorbed gas atoms or molecules was calculated by eq 3.

$$n_1(r) = 4\pi \int_0^{r1} r^2 g(r) \rho \, dr \tag{3}$$

Here $n_1(r)$ is the number of adsorbed gas atoms or molecules in the first layer, $g(r)$ is the RDF, r_1 is the first minimum in the RDF (the position of the first peak in RDF), and ρ is the gas-phase density.

RESULTS AND DISCUSSION

I. Adsorption Isotherms. Figure 2 illustrates the pressure dependence of the number of adsorbed H_2 molecules on the Ag_{256} at four temperatures. This Figure illustrates that the adsorption increases with pressure and gradually reaches a constant value due to the nanocluster surface saturated by a layer of gas atoms, in accordance with adsorption isotherm of Langmuir type I.[4,30] Also, as the results show, increasing the temperature decreases the number of adsorbed molecules. For better comparison, Figure 3 displays the temperature dependence of the number of adsorbed H_2 molecules on the Ag_{38} and Ag_{256}, in a constant H_2 load of 160 H_2 molecules. The number of adsorbed molecules decreases almost exponentially when the temperature increases and reduces significantly at temperatures close to the Ag nanoclusters melting point. This is fundamentally consistent with the fact that higher temperatures give the adsorbates more kinetic energy and this, in turn, results in less chance of being adsorbed. Also, this Figure shows an increase in the number of adsorbed H_2 molecules when cluster size increases at a constant temperature. As cluster size increases, a greater number of atoms are on the surface of the cluster; consequently, the surface of the nanocluster saturates by more gas molecules. The same trends were observed for Xe, Ar, CO, and He gases.

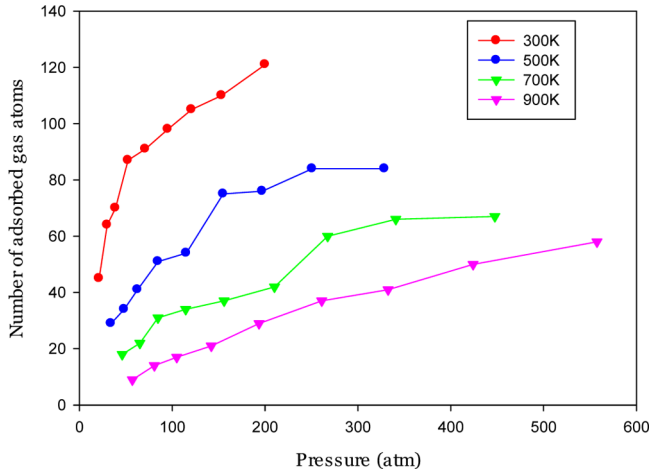

Figure 2. Adsorption isotherms for H_2 on the Ag_{256} nanocluster at four temperatures in various pressures.

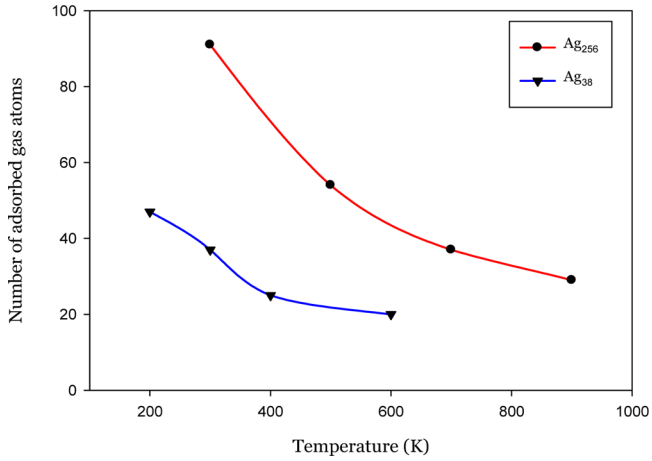

Figure 3. Temperature dependence of the number of adsorbed H_2 molecules on the Ag_{256} and Ag_{38} nanoclusters in the presence of 160 molecules.

Paying attention to the values of L-J parameters (gas−Ag interaction energy) of mentioned gases, it seems that the number of adsorbates should decrease in this trend: Xe > Ar > CO > H_2 > He. However, this trend is not observed in some cases. For example, at the temperature of 300 K, the number of adsorbed atoms on the Ag_{256} nanocluster is 120 for H_2, 94 for CO, 80 for Xe and Ar, and 60 for He. These exceptions can be related to the size and charge effects. At 700 K, the mentioned trend is held true for all gases except for H_2, whereas at 900 K it

dx.doi.org/10.1021/jp407626e | J. Phys. Chem. C 2013, 117, 26287−26294

is true for all of them. At lower temperatures (300 K), more H_2 molecules can be accommodated because of their smaller size (He also has a small size, but its interaction energy with Ag is very low), whereas at higher temperatures (900 K), because of desorption effects, the behavior reverts to the expected trend.

II. Effect of Gas-Phase on the Ag Nanocluster Structure. Figure 4 displays snapshots of graphite-supported

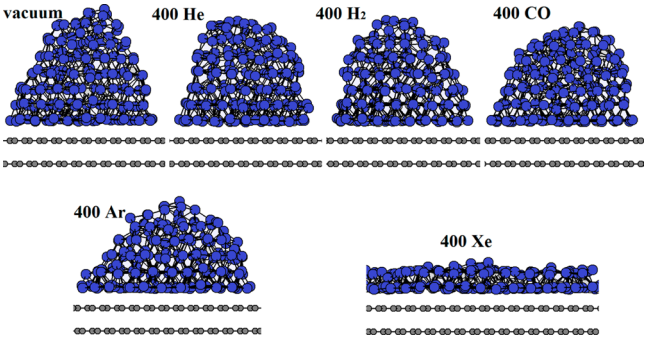

Figure 4. Snapshots of the Ag_{256} nanocluster in the vacuum and in the pressures of various gases at 300 K.

Ag_{256} in the vacuum and in the atmospheres of various gases constituted from 400 gas particles at 300 K. (The gas species have been deleted in picture for clarity.) In contrast with cluster structure under the vacuum conditions, the cluster structure in various gases shows a contraction in the z direction (perpendicular to the graphite surface) and the number of cluster layers decreases. H_2 and He have a smaller effect on the cluster structure, CO and Ar have a greater effect on it, and Xe has the most effect. This phenomenon is expected due to the greater mass of Xe atoms, which leads to larger momentum. Therefore, it exerts a stronger impact on the surface. It can be concluded that the presence of adsorbed gas atoms or molecules exerts a significant effect on the Ag nanocluster surface atoms and has an impact on the overall cluster shape due to the high ratio of surface to bulk atoms in nanoclusters. Therefore, for all of the gases, the interaction between the Ag nanocluster surface atoms and the gas tends to stabilize the surface atoms on the Ag nanocluster.

Also, to examine the structural changes of the nanocluster, we used the density profile (ρ_z) in the z direction (perpendicular to the graphite surface) that was obtained by:

$$\rho_z = \frac{n_z \times \sigma_{Ag-Ag}^3}{\Delta h \times A_{xy} \times N_s} \quad (4)$$

where n_z is the number of Ag atoms in a slice of the simulation box parallel to the xy plane of graphite with a thickness of Δh, A_{xy} is the surface area of the graphite, and N_s is the total number of Ag atoms. Also, σ_{Ag-Ag} is the L-J parameter of Ag.

The density profile (ρ_z) in the z direction (perpendicular to the graphite surface) is shown in Figure 5 for Ag_{256} under various conditions at 300 K. This Figure illustrates that the Ag_{256} has seven layers under the vacuum conditions and in the presence of 400 H_2 molecules and 400 He atoms, six layers in the presence of 400 CO molecules and 400 Ar atoms, and only three layers in the presence of 400 Xe atoms. Also, it can be observed that the peak of the cluster layer adjoining graphite surface increases when the number of layers decreases. The Ag nanocluster surface atoms in the presence of gas species were redistributed to get to a lower energy. Figure 6 shows the

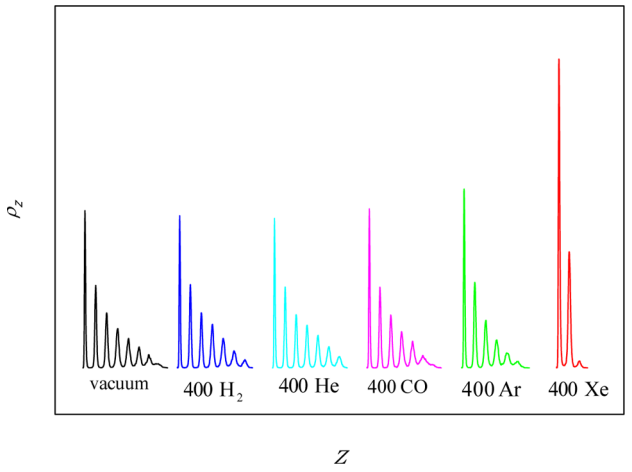

Figure 5. Density profiles in z direction ρ_z of the graphite surface for the Ag_{256} nanocluster in the vacuum and in the pressures of various gases at 300 K. (The substrate locates in the left of each curve.)

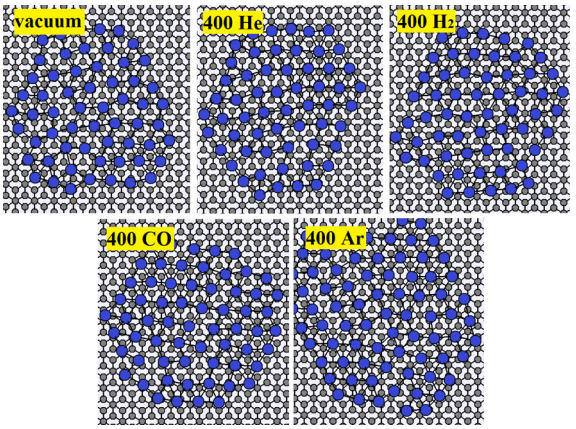

Figure 6. Snapshots of the interface structure of the cluster layer in contact with the substrate for the Ag_{256} at 300 K.

structure of the cluster layer in contact with the graphite surface in the vacuum and in the presence of various gases at 300 K. This Figure illustrates that the Ag atoms in this layer mostly locate on β sites and form rectangular lattices[4,31−33] because the Ag atoms tend to have stronger interactions with C atoms of graphite and make a coherent interface structure. As this Figure shows, in the presence of gas species, the cluster layer in contact with the graphite broadens in comparison with vacuum. (The cluster expands its interface with the substrate.) The average of Ag−Ag bond length in our calculations is 2.65 ± 0.2 Å, which is in good agreement with theoretical[31] and experimental data.[32,33]

Figure 7 shows snapshots of graphite-supported Ag_{256} when the pressure was gradually reduced to zero at 300 K. It can be observed that the nanocluster structure is not similar to its structure in vacuum. (See Figure 4.) It seems that in the presence of gas species the Ag nanocluster structure changes irreversibly and this structure remains stable after the gases are removed. Figure 8 shows this irreversibility using the density profile for Ag_{256} in different loadings of H_2 and Ar at 300 K. The peak of the cluster layer in contact with the graphite surface increases because the cluster prefers to expand its interface with the substrate. It seems that the coherent interface structure between the cluster and the substrate (Figure 6) causes this expansion and the irreversibility of structural

dx.doi.org/10.1021/jp407626e | J. Phys. Chem. C 2013, 117, 26287−26294

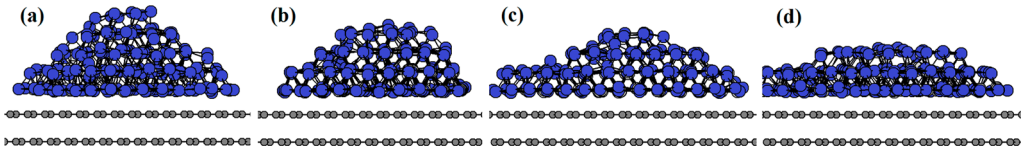

Figure 7. Snapshots of the Ag_{256} nanocluster in the vacuum after exposing to He (a), H_2 (b), CO (c), and Ar (d) at 300 K.

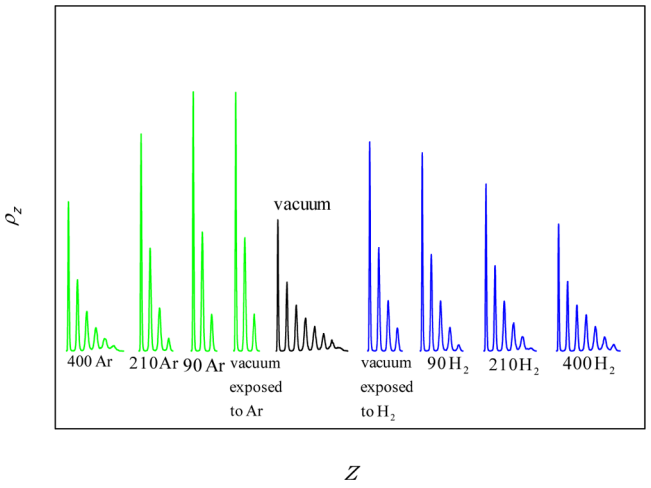

Figure 8. Density profiles in the vacuum (black curve) and in different pressures of H_2 (blue curves) and Ar (green curves) gases at 300 K. (The substrate locates in the left of each curve.)

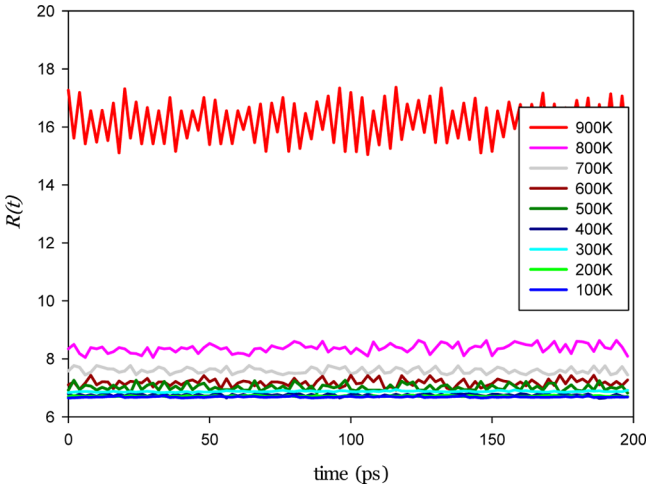

Figure 9. Deformation parameter $R(t)$ for the Ag_{256} nanocluster in vacuum at various temperatures.

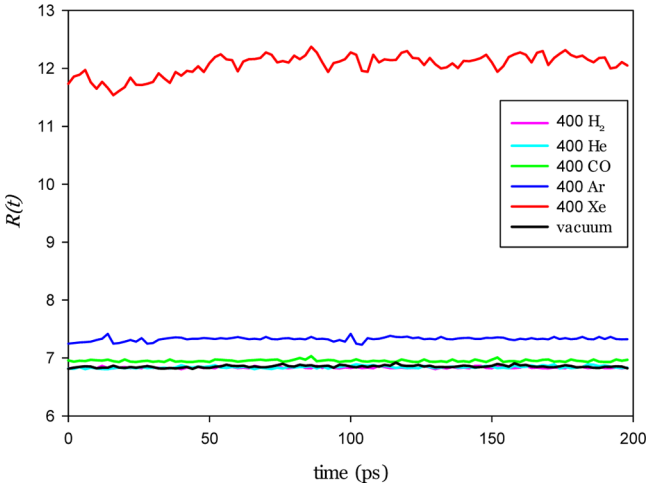

Figure 10. Deformation parameters as a function of various gases for the Ag_{256} at 400 K.

changes. Also, these structural changes modify the surface structure and the nature of the exposed sites. Therefore, the effect of gas atmosphere on the cluster depends on the substrate, temperature, and the nature of the gas.

To investigate the shape evolution of the nanocluster with temperature, we employed the deformation parameter $R(t)$ as an indicator of phase transition of Ag nanoclusters that is defined as:[4]

$$R(t) = \frac{1}{N}\sum_{i=1}^{N}[(X_i(t) - X_{cm}(t))^2 + (Y(t) - Y_{cm}(t))^2 + (Z_i(t) - Z_{cm}(t))^2]^{1/2} \quad (5)$$

Here N is the total number of Ag atoms, X_i, Y_i, and Z_i are the coordinates of the atom i in the x, y, and z directions, the cm subscript exhibits the coordinate of the cluster center of mass, and t shows time evolution.

Figure 9 shows the deformation parameter $R(t)$ for Ag_{256} at time periods of 200 ps. To determine the melting point of the graphite-supported Ag nanoclusters, we calculated the specific heat capacity in constant volume. For all three Ag nanoclusters, the maximum of the specific heat capacity corresponds to their melting point, that is, 420, 620, and 820 K for N = 38, 108, and 256, respectively. At low temperatures, the $R(t)$ has a small value and its fluctuations is low. However, by increasing temperature, the $R(t)$ increases too. Above the melting point (900 K), the shape variation of the cluster as a function of time is much more noticeable. Figure 10 illustrates the variation of deformation parameters of Ag_{256} as a function of various gases at 400 K. It is observed that the effect of gases on the deformation parameter appears to be significantly different in the case of Xe, but for others (He, Ar, CO, and H_2), the deformation parameter is almost similar. The effect of gas atoms on the cluster and Gas-Ag interactions causes the increase in atomic motions within the Ag cluster.

The structure of adsorbed Ar atoms on the cluster layers in the presence of 400 Ar atoms at 300 K is shown in Figure 11. Around the cluster−substrate interface, the gas atoms almost locate amidst the aromatic rings of graphite. As in this site, gas atoms can have stronger interactions with C and Ag atoms. Paying attention to Figure 11, it can be claimed that on average each gas atom has interactions with two Ag atoms and bridge-type coordinations are found between the Ar atoms and the Ag atoms located at the boundary of each layer of the cluster. The adsorbed gas atoms make an ordered layer around the cluster, and in the top cluster layer the gas atoms have one-to-one gas−Ag coordination.

dx.doi.org/10.1021/jp407626e | J. Phys. Chem. C 2013, 117, 26287−26294

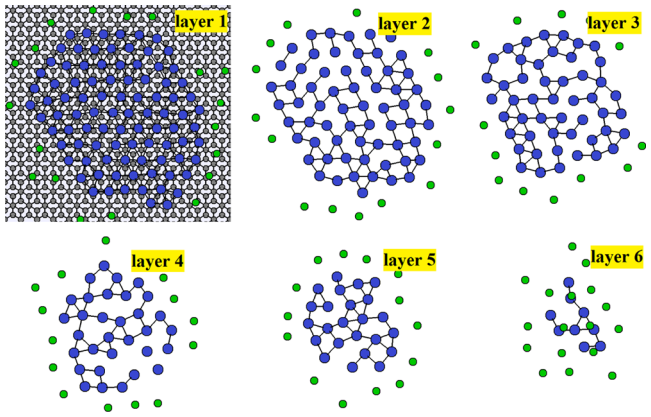

Figure 11. Structure of adsorbed gas atoms around the layers of the Ag_{256} nanocluster in the presence of 400 Ar atoms at 300 K.

III. Dynamics of the Ag Nanoclusters. To study the dynamics of Ag nanoclusters, we employed the mean-square displacement (the MSD of the cluster center of mass) and self-diffusion coefficient (D) for nanoclusters in the vacuum and in gas atmospheres. To study the dynamics of Ag nanoclusters, the MSD and self-diffusion coefficient (D) were obtained by:

$$\mathrm{MSD}(t) = \frac{1}{2}\sum_{i=1}^{N} (|r_i(t + \Delta t) - r_i(t)|)^2 \quad (6)$$

$$D = \frac{1}{6}\lim_{t\to\infty} \frac{\mathrm{d}}{\mathrm{d}t}(\mathrm{MSD}) \quad (7)$$

where $r_i(t)$ is the vector position of the atom i at time and N is the number of atoms of the nanocluster.

The MSD is a combination of how far the nanocluster has moved on the graphite surface and how the atoms inside the nanocluster have moved. Two types of different forces cause these movements. The first type of the forces arises from the nanocluster−graphite interactions, and the second type arises from the Ag−Ag interactions in the nanocluster itself. As mentioned in the previous section, the Ag nanocluster surface atoms in the presence of gas species were redistributed to create a nanocluster with lower energy. This redistribution changes the nanocluster−graphite interfacial contact area and so the nanocluster−graphite interaction and also changes the structural variation on the cluster surface and so the Ag−Ag interaction. Therefore, when there is more structural evolution in the presence of gas, the MSD value will be greater. Figure 12 shows the MSD of Ag_{256} as a function of simulation time at 300 and 500 K under different conditions. At 300 K, the MSD plot has a small slope in vacuum. The plots in the presence of gas atoms or molecules lie above it and with greater slopes. However, Xe gas is more different from others.[4,34] At 500 K, the values of MSD are much higher for all cases, and the difference between the MSD of gases is less. This trend also exists at temperatures above the melting point of the nanocluster, and the MSD difference between gases becomes lesser. It may be illustrated that the type of the gas does not have a considerable effect on dynamics of the nanocluster at temperatures above its melting point due to the high atomic motions in liquid phase. Table 2 illustrates D values for the nanocluster at 300 and 500 K under different conditions.

Figure 13 shows the variations of the Ag_{256} MSD for different numbers of Xe atoms at 300 K. It can be observed that the value of MSD reduces by decreasing the number of Xe atoms.

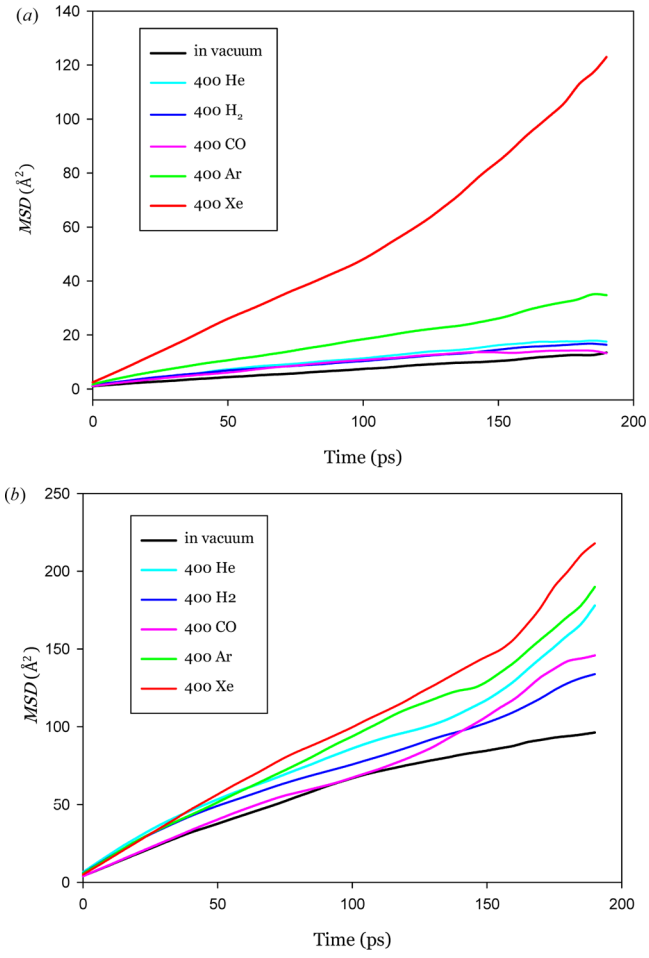

Figure 12. MSD of the Ag_{256} nanocluster in the presence of various gas phases (400 gas atoms) at 300 (a) and 500 K (b).

Table 2. Self-Diffusion Coefficient of Ag_{256} Nanocluster at 300 and 500 K under Different Conditions

	D (cm²/s)	
various conditions	300 K	500 K
vacuum	1.09292×10^{-6}	8.09632×10^{-6}
400 Xe	1.05689×10^{-5}	1.86795×10^{-5}
400 Ar	2.92821×10^{-6}	1.40226×10^{-5}
400 He	1.63569×10^{-6}	1.50427×10^{-5}
400 CO	1.49715×10^{-6}	1.24536×10^{-5}
400 H_2	1.39729×10^{-6}	1.12316×10^{-5}

Initially, this decrease is greater and then gradually becomes less by removing Xe atoms (because the structural evolution in the presence of 400 Xe atoms is more than other Xe atom loadings).

Figure 14 shows the mobility of Ag_{256} on the graphite surface in vacuum (left) and in the presence of 400 Xe atoms (right) at 300 K. The cluster center of mass was monitored in time periods of 100 ps at 300 K in both mentioned conditions by plotting the mobility of center of mass in the x and y directions. Calculations illustrate that the mobility of the cluster on the graphite surface is very different at the two states (in vacuum and in pressure of 400 Xe atoms).

dx.doi.org/10.1021/jp407626e | J. Phys. Chem. C 2013, 117, 26287−26294

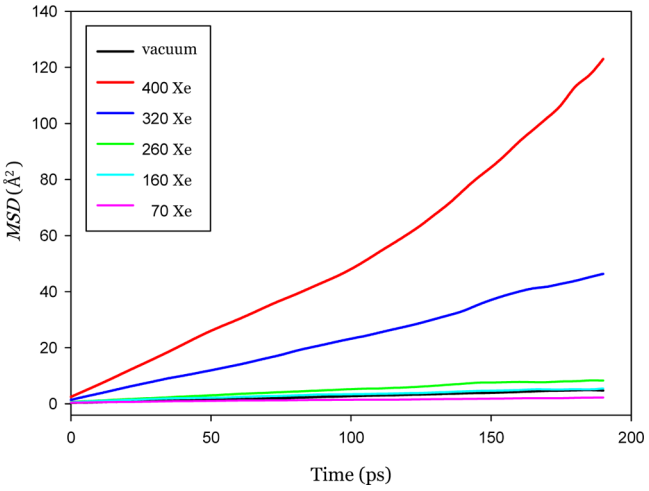

Figure 13. Variations of the MSD of the Ag_{256} nanocluster for different number of Xe atoms at 300K.

CONCLUSIONS

We investigated the adsorption of He, Ar, Xe, CO and H_2 gases and their effects on structural and dynamic properties of the graphite-supported Ag nanoclusters. The results demonstrate that the adsorption of gases on the cluster surface follows the adsorption isotherm of Langmuir type I. Also, the number of adsorbed gas atoms decreases by increasing temperature, in such a way that this decrease is more considerable around and above the melting point of the nanocluster. Also, the adsorption of gases decreases with cluster size due to the decrease in the cluster surface with size.

In general, the gas phase changes the cluster structure and causes the cluster to broadens on the graphite surface. When the pressure is reduced, the cluster retains its structure. So the structural changes due to the presence of the gas phase are identified as irreversible. The gaseous adsorbates make an ordered layer of atoms around the cluster surface and locate at the positions that can have stronger interactions with two Ag atoms, but on the top layer of the cluster the gas atoms have a one-to-one Ag–gas coordination.

Furthermore, the gas phase changes the dynamic properties of the cluster. The gas phase at high pressures increases the mean-square displacement and diffusivity of the cluster significantly. When the pressure decreases, the MSD of the cluster reduces, too, and gradually with decreasing pressure MSD tends to its value in the vacuum. It is found that the type of the gas phase, pressure, temperature, and the cluster size affect the adsorption, structural changes, and dynamical properties of the substrate-supported metallic nanoclusters.

AUTHOR INFORMATION

Corresponding Author

*E-mail: akbarzadehhamed@yahoo.com. Tel: +98 915 3008670. Fax: +98 571 4003323.

Notes

The authors declare no competing financial interest.

REFERENCES

(1) Baletto, F.; Ferrando, R. Structural properties of nanoclusters: Energetic, Thermodynamic, And Kinetic Effets. *Rev. Mod. Phys.* **2005**, *77*, 371–423.

(2) Zhang, Q.; Xie, J.; Yu, Y.; Lee, J. Y. Monodispersity Control In The Synthesis Of Monometallic And Bimetallic Quasi-Spherical Gold And Silver Nanoparticles. *Nanoscale* **2010**, *2*, 1962–1975.

(3) Perez, D. P. *Silver Nanoparticles*; In-Tech: Vukovar, Croatia, 2010.

(4) Lamas, E. J.; Balbuena, P. B. Adsorbate Effects On Structure And Shape Of Supported Nanoclusters: A Molecular Dynamics Study. *J. Phys. Chem. B* **2003**, *107*, 11682–11689.

(5) Wang, Z. L. Transmission Electron Microscopy Of Shape-Controlled Nanocrystals And Their Assemblies. *J. Phys. Chem. B* **2000**, *104*, 1153–1175.

(6) Sun, Y.; Xia, Y. Shape-Controlled Synthesis Of Gold And Silver Nanoparticles. *Science* **2002**, *298*, 2176–2179.

(7) Xu, R.; Wang, D.; Zhang, J.; Li, Y. Shape-Dependent Catalytic Activity Of Silver Nanoparticles For The Oxidation Of Styrene. *Chem. Asian J.* **2006**, *1*, 888–893.

(8) Somorjai, G. A.; Li, Y. *Introduction to Surface Chemistry and Catalysis*; John Wiley and Sons, Inc.: New York, 1994.

(9) Henry, C. R.; Chapon, C.; Duriez, C.; Giorgio, S. Growth And Morphology Of Palladium Particles Epitaxially Deposited On A MgO(100) Surface. *Surf. Sci.* **1991**, *253*, 177–189.

(10) Bazin, D.; Mottet, C.; Tréglia, G. New Opportunities To Understand Heterogeneous Catalysis Processes On Nanoscale Bimetallic Particles Through Synchrotron Radiation And Theoretical Studies. *Appl. Catal., A* **2000**, *200*, 47–54.

(11) Graoui, H.; Giorgio, S.; Henry, C. R. Shape Variations Of Pd Particles Under Oxygen Adsorption. *Surf. Sci.* **1998**, *417*, 350–360.

(12) Hansen, P. L.; Wagner, J. B.; Helveg, S.; Rostrup-Nielsen, J. R.; Clausen, B. S.; Topsøe, H. Atom-Resolved Imaging Of Dynamic Shape Changes In Supported Copper Nanocrystals. *Science* **2002**, *295*, 2053–2055.

(13) Wu, G.-W.; Chan, K.-Y. Molecular Simulation Of Oxygen On Supported Platinum Clusters. *J. Electroanal. Chem.* **1998**, *450*, 225–231.

(14) Ju, S.-P. A Molecular Dynamics Simulation Of The Adsorption Of Water Molecules Surrounding An Au Nanoparticle. *J. Chem. Phys.* **2005**, *122*, 094718-1–094718-6.

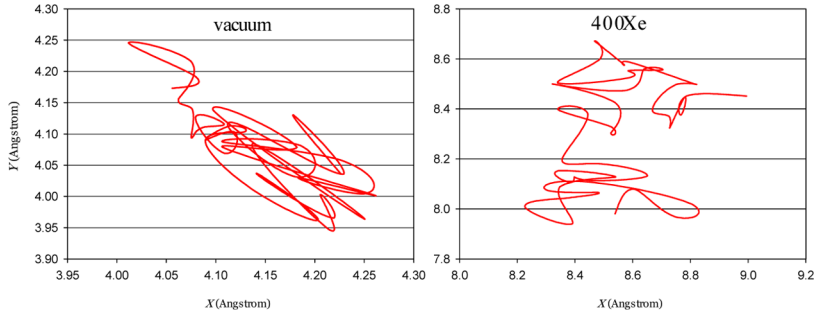

Figure 14. Mobility of the Ag_{256} nanocluster on the graphite surface in vacuum and in the presence of 400 Xe atoms at 300 K.

(15) Berendsen, H. J. C.; Postma, J. P. M.; van Gunsteren, W. F.; Dinola, A.; Haak, J. R. Molecular Dynamics With Coupling To An External Bath. *J. Chem. Phys.* **1984**, *81*, 3684−3690.
(16) Allen, M. P.; Tildesley, D. J. *Computer Simulation of Liquids*; Oxford University Press: Oxford, U.K., 1987.
(17) Smith, W.; Todorov, I. T. A Short Description Of DL_POLY. *Mol. Simul.* **2006**, *32*, 935−943.
(18) Parsafar, G. A.; Spohr, H. V.; Patey, G. N. An Accurate Equation Of State For Fluids And Solids. *J. Phys. Chem. B* **2009**, *113*, 11977−11987.
(19) Sutton, A. P.; Chen, J. Long-range Finnis−Sinclair potentials. *Philos. Mag. Lett.* **1990**, *61*, 139−146.
(20) Uppenbrink, J.; Wales, D. J. Structure And Energetics Of Model Metal Clusters. *J. Chem. Phys.* **1992**, *96*, 8520−8534.
(21) Finnis, M. W.; Sinclair, J. E. A Simple Empirical *N*-Body Potential For Transition Metals. *Philos. Mag. A* **1984**, *50*, 45−55.
(22) Lindsay, L.; Broido, D. A. Optimized Tersoff and Brenner Empirical Potential Parameters For Lattice Dynamics And Phonon Thermal Transport In Carbon Nanotubes And Graphene. *Phys. Rev. B* **2010**, *81*, 205441−205446.
(23) Huarte-Larrañaga, F.; Albertí, M. A Molecular Dynamics Study Of The Distribution Of Molecular Hydrogen Physisorbed On Single Walled Carbon Nanotubes. *Chem. Phys. Lett.* **2007**, *445*, 227−232.
(24) Sirjoosingh, A.; Alavi, S.; Woo, T. K. Grand-Canonical Monte Carlo And Molecular Dynamics Simulations Of Carbon-Dioxide And Carbon-Monoxide Adsorption In Zeolitic Imidazolate Framework Materials. *J. Phys. Chem. C* **2010**, *114*, 2171−2178.
(25) Neek-Amal, M.; Asgari, R.; Rahimi Tabar, M. R. The Formation Of Atomic Nanoclusters On Graphene Sheets. *Nanotechnology* **2009**, *20*, 135602 (1−8)..
(26) Poling, B. E.; Prausnitz, J. M.; O'cannell, J. P. *The Properties of Gases and Liquids*, 5th ed.; McGraw-Hill Companies, Inc.: New York, 2001.
(27) Simon, J.-M.; Haas, O.-E.; Kjelstrup, S. Adsorption And Desorption Of H_2 On Graphite By Molecular Dynamics Simulations. *J. Phys. Chem. C* **2010**, *114*, 10212−10220.
(28) Spruit, M. E. M.; Van Den Hoek, P. J.; Kuipers, E. W.; Geuzebroek, F. H.; Kleyn, A. W. Direct Inelastic Scattering Of Superthermal Ar, CO, NO and O_2 from Ag(111). *Surf. Sci.* **1989**, *214*, 591−615.
(29) Yu, C.; Birgitta Whaley, K.; Hogg, C. S.; Sibener, S. J. Investigation Of The Spatially Isotropic Component Of The Laterally Averaged Molecular Hydrogen/Ag(111) Physisorption Potential. *J. Chem. Phys.* **1985**, *83*, 4217−4234.
(30) Balbuena, P. B.; Gubbins, K. E. Theoretical Interpretation Of Adsorption Behavior Of Simple Fluids In Slit Pores. *Langmuir* **1993**, *9*, 1801−1814.
(31) Rafii-Tabar, H.; Kamiyama, H.; Cross, M. Molecular Dynamics Simulation Of Adsorption Of Ag Particles On A Graphite Substrate. *Surf. Sci.* **1997**, *385*, 187−199.
(32) Ganz, E.; Sattler, K.; Clarke, J. Scanning Tunneling Microscopy Of The Local Atomic Structure Of Two-Dimensional Gold And Silver Islands On Graphite. *Phys. Rev. Lett.* **1988**, *60*, 1856−1859.
(33) Ganz, E.; Sattler, K.; Clarke, J. Scanning Tunneling Microscopy Of Cu, Ag, Au And Al Adatoms, Small Clusters, And Islands On Graphite. *Surf. Sci.* **1989**, *219*, 33−67.
(34) Jalili, S.; Mochani, C.; Akhavan, M.; Schofield, J. Molecular Dynamics Simulation Of A Graphite-Supported Copper Nanocluster: Thermodynamic Properties And Gas Adsorption. *Mol. Phys.* **2012**, *110*, 267−276.